

Zirconia-based composites with tailored composition and architecture: elaboration and microstructural characterization

Marta Fornabaio¹, Rebecca Traverso¹, Paola Palmero¹, Helen Reveron², Jérôme Chevalier^{2,3} and Laura Montanaro¹

¹ Department of Applied Science and Technology, INSTM R.U. PoliTO, LINCE Lab., Politecnico di Torino, Corso Duca degli Abruzzi, 24, 10129 Torino, Italy

² Université de Lyon, INSA de Lyon, MATEIS UMR CNRS 5510, Bât. Blaise Pascal 7, Av. Jean Capelle, 69621 Villeurbanne, France

³ Institut Universitaire de France, 103 bd Saint-Michel, 75005 Paris, France

Abstract

This research was carried out in the frame of the European Project called *Longlife*, whose focus is the development of ceramic dental and spine implants, characterized by enhanced reliability and lifetime as compared to the current devices. In this context, we have developed innovative zirconia-based composites, in which equiaxial α -Al₂O₃ and elongated SrAl₁₂O₁₉ phases are dispersed in a ceria-stabilized zirconia matrix. The composite powders were prepared by a surface coating route, in which commercial zirconia powders are coated by inorganic precursors of the second phases. Even if simple, this process requires the careful control of many processing steps, such as the dispersion conditions and the pH of the suspension. Samples containing four different ceria contents (in the range 10.0-11.5 mol%) were prepared by carefully tailoring the amount of the cerium precursor during the elaboration process. Slip cast green bodies were sintered at 1450°C for 1 h, leading to fully dense materials. The microstructural characterization showed very homogeneous microstructures with an even distribution of both equiaxial and elongated-shaped grains inside a fine zirconia matrix.

Keywords: Zirconia-based composites, Phase composition, Microstructure

1 Introduction

Inert bioceramics, such as alumina and yttria-stabilized zirconia (Y-TZP), have been successfully used as components for orthopaedic and dental applications, due to their biocompatibility, mechanical properties and aesthetics. Unfortunately, alumina exhibits two major concerns when used for load-bearing applications: the low fracture toughness and the susceptibility to failure by slow crack growth, occurring under stresses well below the fracture strength [1].

On the other side, Y-TZP presents excellent mechanical properties [2], beside good aesthetics and biocompatibility characteristics. However, some Y-TZP compositions present poor *in vivo* stability, which limits their application in the biomedical field [3]. Therefore, current research is now focusing on alternative zirconia-based materials characterized by a reduced susceptibility to ageing. The most promising material is ceria-stabilized zirconia (Ce-TZP) [4], characterized by a higher stability as compared to Y-TZP, but by a significantly lower strength [5]. Therefore, in order to increase the mechanical properties of Ce-TZP is essential to move to composite systems [6], being the search for new compositions and architectures the current trend for reaching increasingly better properties [7]. However, it is essential to tailor the microstructure, and hence the processing, to achieve the expected properties and to fulfill the requirements for biomedical applications.

Zirconia-based composite powders are traditionally produced by the milling and mixing method or by wet chemical routes. Recently, a novel processing route has been developed [8-10] based on coating the surface of a commercial powder with precursors of the second phase. The close mixing between the matrix ceramic particles and the precursor is realized at nano/atomic level, assuring an excellent distribution of the second phase in the composite material. Despite the surface coating methods so far reported [8,9] the method described in this study implies the use of only inorganic precursors and aqueous media, thus reducing processing costs and environmental impacts.

2 Materials and Methods

A commercial 10 mol% ceria-stabilized zirconia powder (supplied by Daiichi Kigenso Kagaku Kogio Co. LTD, Japan, referred to as 10Ce-TZP) was employed as raw material to develop composite powders having the following composition: 84 vol% ZrO_2 - 8 vol% Al_2O_3 - 8 vol% $SrAl_{12}O_{19}$ (referred to as ZA_8Sr_8).

As-received and calcined 10Ce-TZP powders were submitted to XRD analysis (Philips PW3830). The Toraya equation [11] was used to determine the monoclinic volume fraction (V_m), whereas the Scherrer equation [12] was used to estimate the crystallite size.

The as-received and calcined powders were dispersed by ball milling by using 2 mm-diameter zirconia spheres. The starting suspension pH (about 6.5) was modified by adding diluted hydrochloric acid to reach a final pH value of 3. The evolution of the particle size distribution within the dispersion time was determined by laser granulometry (Fritsch model Analysette 22 Compact), whereas the possible release of ceria from the stabilized zirconia powders was investigated by ICP-AES analysis (Optima 2100, Perkin Elmer). In particular, the slurries were centrifuged for separating the solid powder from the supernatant liquid phase, which was analyzed.

When dispersed, the zirconia slurries were mixed with the nitrates aqueous solutions. $Al(NO_3)_3 \cdot 9H_2O$ (>98% purity, Sigma-Aldrich) and $Sr(NO_3)_2$ (>99.0% purity, Sigma-Aldrich) were used as aluminum and strontium precursors, respectively. In some synthesis, different amounts of ammonium cerium nitrate $((NH_4)_2[Ce(NO_3)_6]$, $\geq 98.5\%$ purity, Sigma-Aldrich) were also added in order to increase the starting ceria content (10 mol%) to 10.5, 11.0 and 11.5 mol%, respectively. The modified suspensions were kept under magnetic stirring for 2 h and finally spray-dried. The doped powders were pre-treated at 600°C for 1 h for inducing the decomposition of the by-products. In addition, a second pre-treatment was carried out at 1150°C, to induce the crystallization of the second phases on the zirconia particle surface. For sake of clarity, a scheme of the process has been reported in Figure 1.

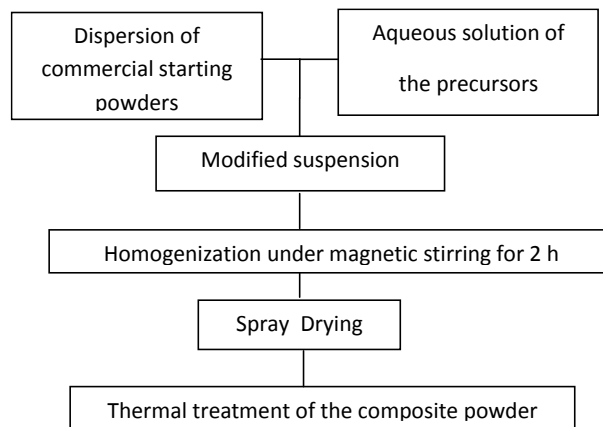


Fig. 1: Flow chart of the adopted procedure for the composite powder elaboration

Green bodies were prepared by slip casting: aqueous suspensions at solid loading of 26 vol% were dispersed by ball-milling for about 30 h. The fired materials were obtained by pressureless sintering at 1450°C for 1 h.

The green and fired densities were evaluated by mass-geometric measurements and Archimedes method and referred to the materials theoretical density (TD), calculated by the rule of mixtures for composite systems. The phase composition was investigated by XRD. The microstructures were analyzed by means of scanning electron microscopy (SEM Zeiss SUPRA VP55) on polished and thermally etched specimens. The mean grain sizes of matrix and second phases were determined by image analysis (Scandium Soft imaging system software).

3 Results and Discussion

The XRD pattern of the as-received 10Ce-TZP is depicted in Figure 2 (a). We can observe that the powder is a mixture of monoclinic and tetragonal zirconia phase, being V_m about 68%.

Figure 2 (b) shows the evolution of V_m as well as of the zirconia crystallite size as a function of the powder thermal treatment. V_m (Figure 2(b), bottom) progressively decreases by increasing the calcination temperature, reaches a minimum at about 950°C (with 1 h of holding time) and then increases again by increasing the heating temperature. The mean crystallite size of the starting 10Ce-TZP was about 25 nm (Figure 2(b), top) and remained almost constant up to about 950°C. For higher temperatures, it started to increase, reaching values of about 50 nm after calcination at 1500°C. These results show that in the temperature range from 900 to 950°C the lowest values for both monoclinic fraction and crystallite size can be obtained.

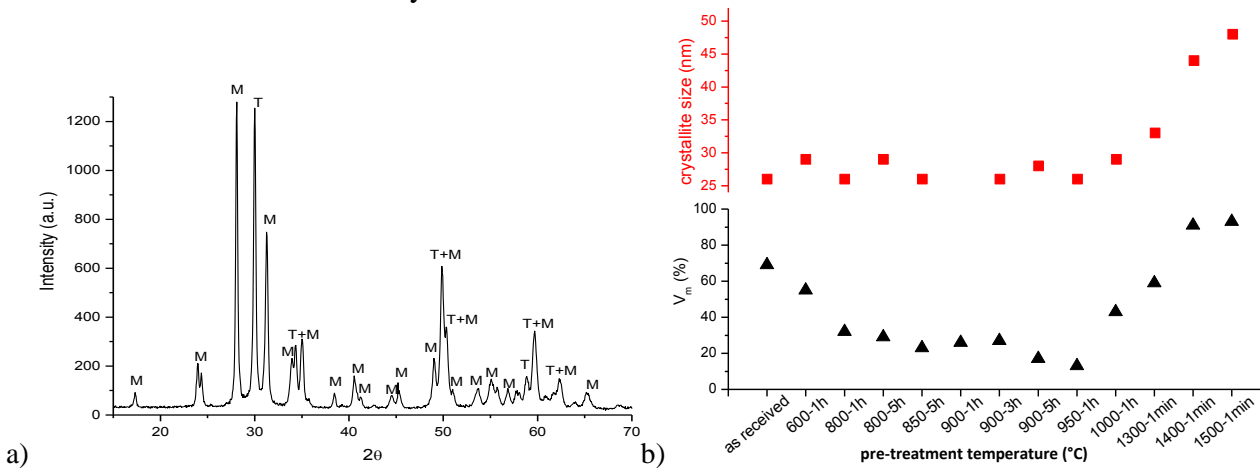


Fig. 2 (a): XRD pattern of the as-received 10Ce-TZP; (b): V_m (bottom) and zirconia crystallite size (top) as a function of the calcination treatments.

As-received 10Ce-TZP was characterized by a certain agglomeration, being the mean agglomerate size of about 1 μm (Figure 3). Thus, it was necessary to disperse the powder, since a good de-agglomeration degree is a key requirement to achieve a close and homogeneous contact between the matrix powder and the metal precursors of the second phases.

The dispersion conditions were set-up according to the Zeta-potential curves reported in literature for zirconia and ceria-stabilized zirconia powders [13], which attest that the isoelectric point was in the pH range 7-8. According to these data, both acid and basic dispersion conditions can be selected. By keeping in mind that the subsequent elaboration steps require an acid environment (addition with the metal nitrate solution, as shown in the flow chart of Figure 1), we decided to disperse the powder under acid conditions (pH 3). At the same time, cerium could be solubilised in

a certain extent in acid medium, as shown in literature [14], inducing an undesired depletion of the zirconia lattice.

In order to limit as much as possible the above drawback, we carried out the acid dispersion both on as-received 10Ce-TZP and on powders submitted to calcination treatments, characterized by a higher fraction of tetragonal phase, thus attesting a more effective stabilization from the cerium oxide. On the ground of the results collected in Figure 3, two calcination treatments were selected: 900°C/1h and 950°C/1h, respectively. In fact, at these temperatures, relatively low V_m and fine zirconia crystallite size have been determined.

Figure 3 collects the cumulative size distribution curves of 10Ce-TZP and of the same powder calcined at 900°C and at 950°C. After 16 hours of ball-milling at pH 3, all three powders reached a good de-agglomeration degree, being the average particle size of about 0.5 μm .

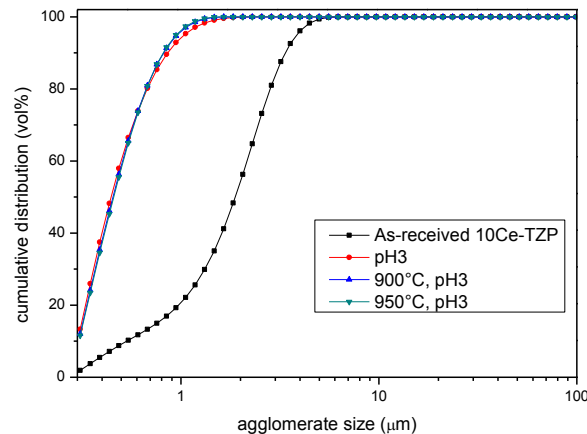


Fig. 3: Cumulative frequency (vol%) of the as-received (black curve), dispersed (red curve), calcined and dispersed (900°C, blue curve; 950°C, green curve) 10Ce-TZP powders.

In Figure 4, FESEM micrographs of the three dispersed powders are collected: we can observe similar microstructural features: the three powders show agglomerates of 200-800 nm in size, in which primary particles of about 50 nm can be clearly identified. By this observation, it appears that the thermal treatment did not induce grain growth.

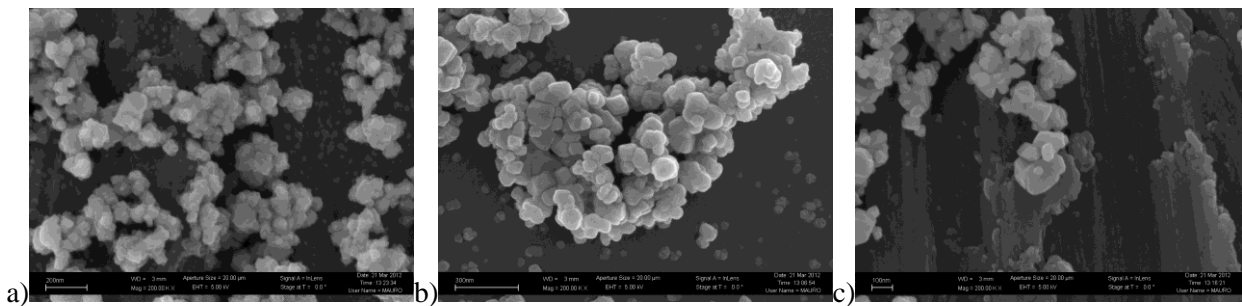


Fig. 4: FESEM micrographs of as-received (a), calcined at 900°C (b) and calcined at 950°C (c) 10Ce-TZP powders, after dispersion under acid conditions.

By ICP-AES analysis, the cerium concentration in the liquid phase was lower than the instrumental detection limit, for all three powders. This result confirms the lack of cerium release during the dispersion under acid conditions. According to this result, the composite powders were prepared by using un-calcined 10Ce-TZP powders.

The surface coating method was successful in yielding the desired composition: in fact, the XRD analyses performed on the sintered materials, having different ceria contents (Figure 5), showed the

presence of tetragonal and monoclinic zirconia phases as well as of α -Al₂O₃ and SrAl₁₂O₁₉ phases. In addition, V_m decreased as the ceria content increased: V_m was in fact 7, 5, 3 and 1 vol% for zirconia powders containing 10.0, 10.5, 11.0 and 11.5 mol% of ceria, respectively. This result suggests that the surface coating process allows tailoring the ceria amount inside the zirconia grains in a very effective way: the lower the ceria content during synthesis, the higher the monoclinic fraction after sintering.

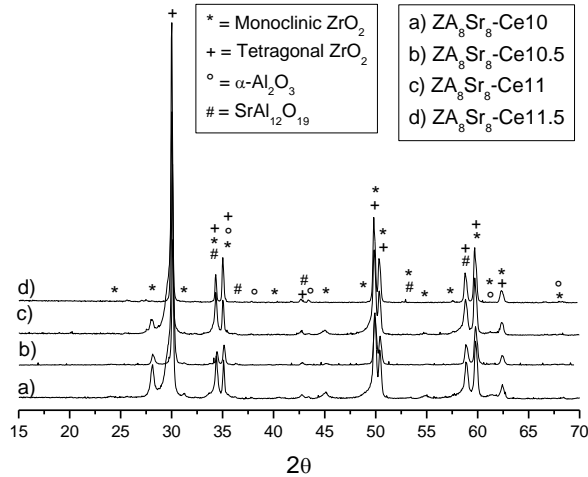


Fig. 5: XRD patterns of sintered ZA₈Sr₈ containing 10.0 (a), 10.5 (b), 11.0 (c) and 11.5 (c) mol% ceria

The microstructure of the material containing 11mol% of ceria is depicted in Figure 6. A completely homogeneous and dense microstructure with an even distribution of all the phases inside the composite materials was observed, whatever the ceria content. The second phase particles had the desired morphology, both rounded (α -Al₂O₃ phase) and elongated (SrAl₁₂O₁₉ phase). By image analysis we determined an average particle size of 0.6 ± 0.2 μm and of 0.3 ± 0.1 μm for zirconia and alumina grains, respectively. The strontium hexaaluminate grains were characterized by mean length of 0.6 ± 0.2 μm and aspect ratio of 5 ± 2 . The same microstructural features can be observed in samples containing different ceria amounts.

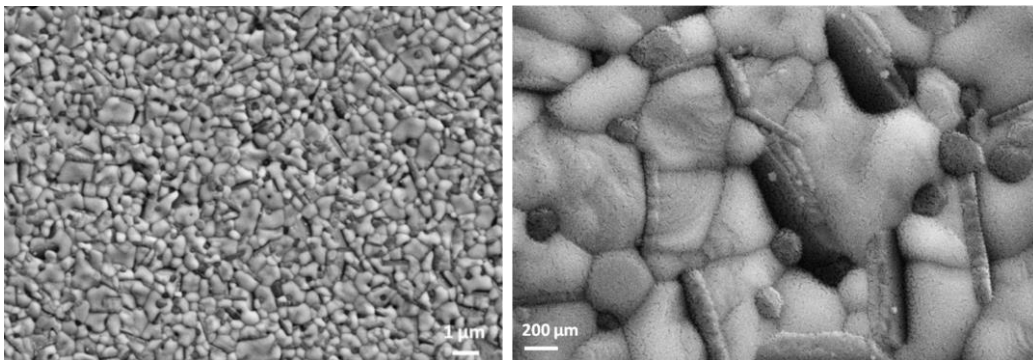


Fig. 6: SEM micrographs of the microstructure of ZA₈Sr₈ containing 11.0 mol% ceria, sintered at 1450°C/1h

4 Conclusions

In order to fulfill the clinical requirements for strong, tough and stable ceramics, three-phase composite materials were developed. Both equiaxed (α -Al₂O₃) and elongated (SrAl₁₂O₁₉) second phases were added to the ceria-stabilized zirconia matrix (10Ce-TZP). In addition, extra-ceria was added to some samples with the aim of producing sintered materials with cerium oxide in the range

10.0–11.5 mol%. The composite powders were produced by a simple but reliable surface coating process, in which zirconia powders were coated by inorganic precursors of the second phases, which crystallize on the zirconia particles surface under proper thermal treatment. This method allows precise tuning of many compositional and microstructural features simultaneously in the final nanocomposite structures. The microstructures are fully homogeneous with optimal distribution of both second phases in the zirconia matrix. Moreover, the process allows fine tuning of the ceria content in the zirconia lattice, thus highlighting the potential of the proposed process to produce appropriate composites for biomedical applications.

5 Reference list

- [1] Rahaman M.N., Yao A., Bal B.S.; Garino J.P., Ries, M.D.: Ceramics for Prosthetic Hip and Knee Joint Replacement, *J Am Ceram Soc*, Vol. 90, 2007, pp. 1965-88.
- [2] Fisher J., Stawarczyk B.: Compatibility of machined Ce-TZP/Al₂O₃ nanocomposite and a veneering ceramic, *Dent Mater*, Vol. 23, 2007, pp. 1500-5.
- [3] Chevalier J., Gremillard L., Virkar A.V., Clarke D.R.: The Tetragonal-Monoclinic Transformation in Zirconia: Lesson Learned and Future Trends, *J Am Ceram Soc*, Vol. 92, 2009, pp. 1901-20.
- [4] Chevalier J., Gremillard L.: Ceramics for medical applications: A picture for the next 20 years, *J Eur Ceram Soc*, Vol. 29, 2009, pp. 1245-55.
- [5] El Attaoui H., Saâdaoui M., Chevalier J., Fantozzi G.: Static and cyclic crack propagation in Ce-TZP ceramics with different amounts of transformation toughening, *J Eur Ceram Soc*, Vol. 27, 2007, pp. 483-86.
- [6] Nawa M., Nakamoto S., Sekino T., Niihara K.: Tough and strong Ce-TZP/Alumina nanocomposites doped with Titania. *Cer Int*, Vol. 24, 1998, pp. 497-506.
- [7] Cutler R.A., Lindemann J.M., Ulvensoen J.H., Lange H.I.: Damage-Resistant SrO-Doped Ce-TZP/Al₂O₃ Composites, *Mater Design*, Vol. 15, 1994, pp. 123-33.
- [8] Schehl M., Diaz J.A., Torrecillas R.: Alumina nanocomposites from powder-alkoxide mixtures, *Acta Materialia*, Vol. 50, 2002, pp. 1125-39.
- [9] Yuan Z., Vleugels J., Van Der Biest O.: Synthesis and characterization of CeO₂-coated ZrO₂ powder-based TZP, *Mater Lett*, Vol. 46, 2000, pp. 249-54.
- [10] Palmero P., Naglieri V., Chevalier J., Fantozzi G., Montanaro L.: Alumina-based nanocomposites obtained by doping with inorganic salt solutions: Application to immiscible and reactive systems, *J Eur Ceram Soc*, Vol. 29, 2009, pp. 59-66.
- [11] Toraya H., Yoshimura M., Somiya S.: Calibration curve for quantitative analysis of the monoclinic-tetragonal ZrO₂ system by X-Ray diffraction, *J Amer Ceram Soc*, Vol. 67, 1984, pp. C119-21.
- [12] Patterson, A.: The Scherrer Formula for X-Ray Particle Size Determination, *Phys Rev*, Vol. 56, 1939, pp. 978–82.
- [13] Fengqiu T.: Effect of dispersants on surface chemical properties of nano-zirconia suspensions, *Ceram Int*, Vol. 26, 2000, pp.93-97.
- [14] Greenwood R., Bergstrom L.: Electroacoustic and Rheological Properties of Aqueous Ce-ZrO₂ (Ce-TZP) Suspensions, *J Eur Ceram Soc*, Vol. 17, 1997, pp.537-48.